JCI The Journal of Clinical Investigation

PKCδ regulates hepatic insulin sensitivity and hepatosteatosis in mice and humans

Olivier Bezy, Thien T. Tran, Jussi Pihlajamäki, Ryo Suzuki, Brice Emanuelli, Jonathan Winnay, Marcelo A. Mori, Joel Haas, Sudha B. Biddinger, Michael Leitges, Allison B. Goldfine, Mary Elizabeth Patti, George L. King, C. Ronald Kahn

J Clin Invest. 2011;121(6):2504-2517. https://doi.org/10.1172/JCI46045.

Research Article **Metabolism**

C57BL/6J and 129S6/Sv (B6 and 129) mice differ dramatically in their susceptibility to developing diabetes in response to diet- or genetically induced insulin resistance. A major locus contributing to this difference has been mapped to a region on mouse chromosome 14 that contains the gene encoding PKCδ. Here, we found that PKCδ expression in liver was 2-fold higher in B6 versus 129 mice from birth and was further increased in B6 but not 129 mice in response to a high-fat diet. *PRKCD* gene expression was also elevated in obese humans and was positively correlated with fasting glucose and circulating triglycerides. Mice with global or liver-specific inactivation of the *Prkcd* gene displayed increased hepatic insulin signaling and reduced expression of gluconeogenic and lipogenic enzymes. This resulted in increased insulin-induced suppression of hepatic gluconeogenesis, improved glucose tolerance, and reduced hepatosteatosis with aging. Conversely, mice with liver-specific overexpression of PKCδ developed hepatic insulin resistance characterized by decreased insulin signaling, enhanced lipogenic gene expression, and hepatosteatosis. Therefore, changes in the expression and regulation of PKCδ between strains of mice and in obese humans play an important role in the genetic risk of hepatic insulin resistance, glucose intolerance, and hepatosteatosis; and thus PKCδ may be a potential target in the treatment of metabolic syndrome.

PKCδ regulates hepatic insulin sensitivity and hepatosteatosis in mice and humans

Olivier Bezy,[1] Thien T. Tran,[1] Jussi Pihlajamäki,[2] Ryo Suzuki,[1] Brice Emanuelli,[1] Jonathan Winnay,[1] Marcelo A. Mori,[1] Joel Haas,[1] Sudha B. Biddinger,[1,3] Michael Leitges,[4] Allison B. Goldfine,[1] Mary Elizabeth Patti,[1] George L. King,[1] and C. Ronald Kahn[1]

[1]Joslin Diabetes Center and Harvard Medical School, Boston, Massachusetts, USA. [2]Departments of Medicine and Clinical Nutrition, University of Eastern Finland and Kuopio University Hospital, Kuopio, Finland. [3]Division of Endocrinology, Children's Hospital Boston, Harvard Medical School, Boston, Massachusetts, USA. [4]Biotechnology Centre of Oslo, University of Oslo, Oslo, Norway.

C57BL/6J and 129S6/Sv (B6 and 129) mice differ dramatically in their susceptibility to developing diabetes in response to diet- or genetically induced insulin resistance. A major locus contributing to this difference has been mapped to a region on mouse chromosome 14 that contains the gene encoding PKCδ. Here, we found that PKCδ expression in liver was 2-fold higher in B6 versus 129 mice from birth and was further increased in B6 but not 129 mice in response to a high-fat diet. *PRKCD* gene expression was also elevated in obese humans and was positively correlated with fasting glucose and circulating triglycerides. Mice with global or liver-specific inactivation of the *Prkcd* gene displayed increased hepatic insulin signaling and reduced expression of gluconeogenic and lipogenic enzymes. This resulted in increased insulin-induced suppression of hepatic gluconeogenesis, improved glucose tolerance, and reduced hepatosteatosis with aging. Conversely, mice with liver-specific overexpression of PKCδ developed hepatic insulin resistance characterized by decreased insulin signaling, enhanced lipogenic gene expression, and hepatosteatosis. Therefore, changes in the expression and regulation of PKCδ between strains of mice and in obese humans play an important role in the genetic risk of hepatic insulin resistance, glucose intolerance, and hepatosteatosis; and thus PKCδ may be a potential target in the treatment of metabolic syndrome.

Introduction

Obesity and type 2 diabetes (T2D) are major health problems worldwide and are projected to further increase in prevalence over the next two decades. Likewise, the closely related metabolic syndrome, with all of its complications, is increasing at epidemic rates. Indeed, nonalcoholic hepatosteatosis is now the second most common cause of chronic liver failure (1). All these disorders are the result of interactions between inherited genetic factors and varying environmental exposures.

Mouse models provide a powerful tool to investigate genetic and environmental components involved in the disease susceptibility. In mice, it has been shown that different genetic backgrounds strongly modify the susceptibility to diet-induced obesity, insulin resistance, hepatic steatosis, β cell failure, and T2D, in some cases in very dramatic ways (2–6). For example, we have previously shown that C57BL/6J and 129S6/Sv (B6 and 129) mice have remarkably different metabolic responses to high-fat diet–induced (HFD-induced) insulin resistance. On regular chow diet, B6 mice gain more weight, have higher levels of insulin and leptin, and show greater glucose intolerance than 129 mice, and these phenotypic differences are further exacerbated with high-fat feeding (6). Likewise, when stressed with genetically induced insulin resistance due to heterozygous deletion of both insulin receptor and insulin receptor substrate 1 (IRS-1), more than 90% of B6 mice develop diabetes, whereas less than 5% of 129 mice carrying this form of genetic insulin resistance become diabetic (5). This difference in development of diabetes between the strains of mice is due to differences in insulin resistance rather than β cell function. Thus, some factor(s) in the genetic differences between B6 and 129 mice are a virtual on-off switch for the development of T2D.

Genome-wide scanning of a F_2 intercross between B6 and 129 mice has identified several quantitative trait loci (QTLs) linked to this difference in development of diabetes (6, 7). The strongest QTL was on chromosome 14 and was linked to the development of hyperinsulinemia and insulin resistance in both genetic and diet-induced insulin resistance. One of the genes in the region showing association with insulin resistance is *Prkcd*, the gene that encodes PKCδ. In previous studies, we also found that PKCδ is differentially expressed in some tissues from B6 and 129 mice (6). *PRKCD* is an interesting candidate gene for the difference in insulin resistance. Several members of the PKC family have been shown to be able to phosphorylate the insulin receptor or IRS-1 and inhibit insulin action (8–10). PKCδ has also been suggested to play a role in fatty acid–induced insulin resistance and regulation of lipogenesis in liver (11, 12).

In the present study, we have explored the potential role of PKCδ as a key genetic modifier of insulin resistance in mice. We found that diabetes-prone B6 mice, and other insulin resistance mouse models, display increased levels of PKCδ expression in liver compared with diabetes-resistant 129 mice, and that upon high-fat feeding, this difference in PKCδ expression increases further due to increases in the B6 mouse. We also find that hepatic PKCδ expression correlates with BMI, fasting glycemia, and circulating triglyceride levels in obese humans. Using PKCδ-null mice, as well as mice with either liver-specific overexpression or liver-specific inactivation of the *Prkcd* gene, we demonstrate that these differences in PKCδ expression serve as an important modifier of hepatic insulin resistance, hepatic steatosis, and the genetic control of insulin resistance between these

Conflict of interest: The authors have declared that no conflict of interest exists.
Citation for this article: *J Clin Invest.* 2011;121(6):2504–2517. doi:10.1172/JCI46045.

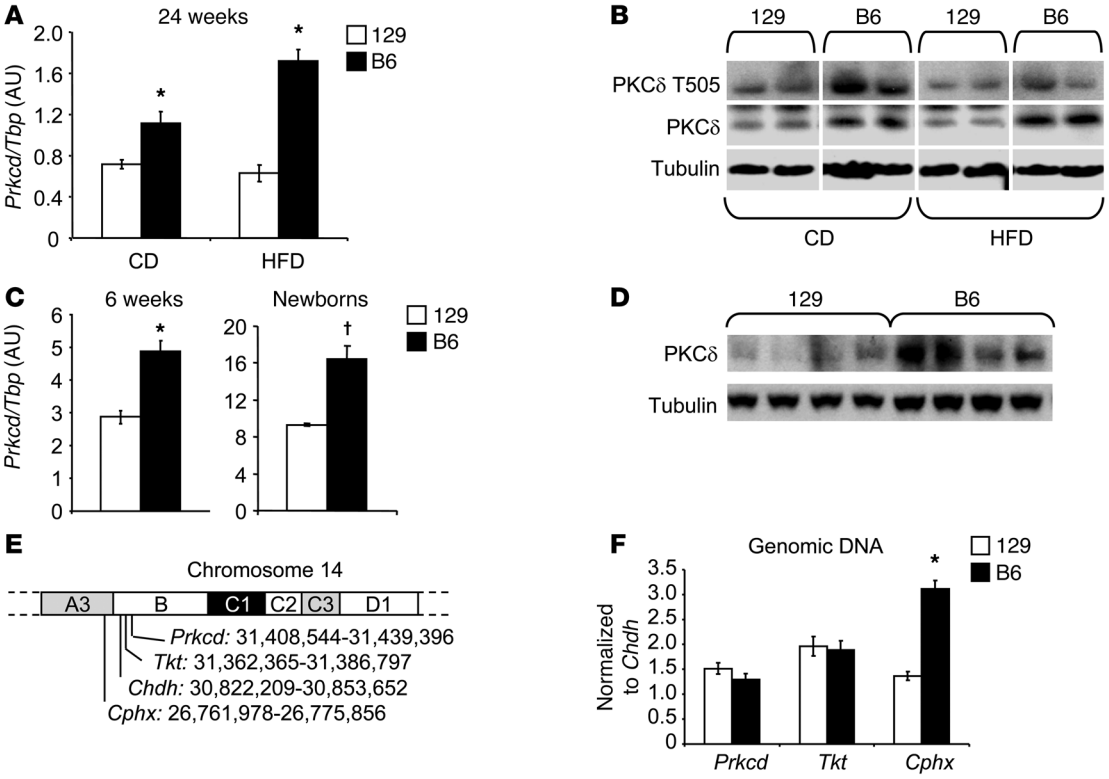

Figure 1

Differential hepatic PKCδ expression between diabetes-susceptible B6 and diabetes-resistant 129 mice. (**A**) Hepatic expression of *Prkcd* mRNA in 24-week-old chow diet– (CD-) versus 18-week HFD-treated B6 and 129 mice. Results are normalized to *Tbp* (n = 8 per group, $^*P < 0.02$). (**B**) Western blot analysis of PKCδ protein expression and phosphorylation on Thr505 in liver of 24-week-old CD- versus 18-week HFD-treated B6 and 129 mice. Lanes were run on the same gel but were noncontiguous. (**C**) *Prkcd* mRNA expression in liver of 6-week-old (n = 5 per group, $^*P < 0.001$) and newborn (n = 7 per group, $^\dagger P < 0.004$) B6 and 129 mice. (**D**) Western blot analysis of PKCδ protein expression in liver of newborn B6 and 129 mice. (**E**) Schematic of *Prkcd*, *Tkt*, *Cphx*, and *Chdh* genes localization on mouse chromosome 14. (**F**) Copy number variation for *Prkcd*, *Tkt*, and *Cphx* genes between B6 and 129 mice lines (n = 6 per group). Results were normalized to *Chdh* ($^*P < 0.00003$).

mouse strains. Together, our data suggest that PKCδ could be an important target for improving insulin sensitivity and preventing development of diabetes and hepatic steatosis in humans with diet-induced obesity.

Results

Increased expression of PKCδ in liver is a feature of pro-diabetic mice. Compared with 129 mice, B6 mice develop more severe insulin resistance when subjected to either a genetic defect in insulin signaling or environmentally induced insulin resistance following HFD feeding. Genome-wide association analysis reveals several regions linked to increased risk of insulin resistance in the B6 mouse, the strongest of which is around the *Prkcd* locus on chromosome 14 (6). This genetic background difference was associated with increased expression of PKCδ in B6 mice. Thus, on a normal chow diet, 24-week-old B6 mice had approximately 60% higher levels of *Prkcd* mRNA in liver than age- and diet-matched 129 mice (1.1 ± 0.1 vs. 0.71 ± 0.04, $P < 0.02$) (Figure 1A). Moreover, when B6 and 129 mice were placed on a HFD from 6 to 24 weeks of age, hepatic *Prkcd* expression further increased by 2-fold in B6 mice, but did not increase in 129 mice, leading to 3-fold higher expression of *Prkcd* in the B6 versus 129 mice (Figure 1A). These differences in mRNA expression led to similar differences in PKCδ expression at the protein level, as assessed by Western blot analysis of liver extracts, which in turn were paralleled by a commensurate increase in PKCδ with phosphorylation on threonine 505 (Figure 1B). This difference in *Prkcd* expression was also observed at 6 weeks of age (Figure 1C), when 129 mice actually weighed slightly more than the B6 mice (22.1 ± 0.5 vs. 19.8 ± 0.3 g, $P < 0.001$) and had identical glucose and insulin levels; and more importantly, it was also observed at both mRNA and protein levels in livers of newborn B6 versus 129 mice (Figure 1, C and D). The results suggest that there is a genetically driven differential expression of PKCδ between the insulin resistance–prone B6 and insulin resistance–resistant 129 mice.

Recent studies have revealed that one cause of the differences in gene expression between mouse strains is duplication or deletion of segments of DNA resulting in variation in gene copy number. Copy number variations have been identified in chromosome 14 near the *Prkcd* locus between commonly used mouse lines, including B6 and 129 (13). To explore whether this could account for the differences in expression of PKCδ, we assessed the relative copy number of the *Prkcd* gene and the nearby *Tkt* gene, as well as *Cphx* and *Chdh* genes located upstream and downstream of *Prkcd* on chromosome 14 (Figure 1E). Since the *Chdh* gene is known not to exhibit copy variations, the results for other genes could be normalized to *Chdh* to assess copy number variation. Consistent with previous reports indicating duplication in this region (13), we observed a 2-fold increase in copy number for the *Cphx* gene in

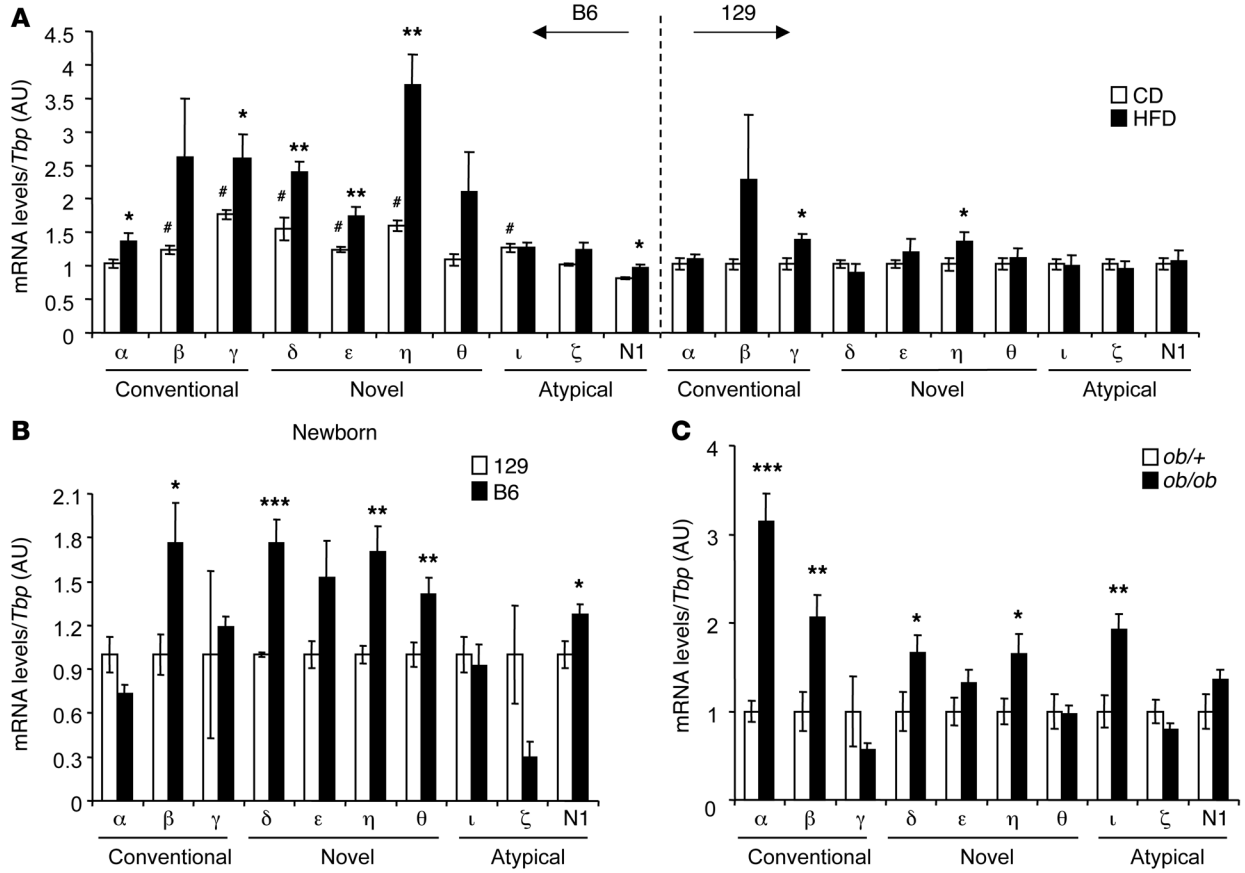

Figure 2
General expression analysis of PKC mRNA in liver of diabetic or diabetes-resistant mouse models. Expression of all PKCs was measured by qPCR in liver of (**A**) 24-week-old CD versus 18-week HFD-treated B6 and 129 mice (n = 8 per group, $^{\#}P < 0.05$, B6 CD compared with 129 CD; $^{*}P < 0.05$, CD compared with HFD); and (**B**) newborn B6 and 129 mice (n = 7 per group, $^{*}P < 0.05$, $^{**}P < 0.01$, $^{***}P < 0.001$). (**C**) *ob*/+ versus *ob*/*ob* mice (n = 9–15 per group, $^{*}P < 0.05$, $^{**}P < 0.01$, $^{***}P < 0.001$). Results are normalized to *Tbp*.

B6 mice compared with 129 mice ($P < 0.0001$). However, genomic PCR revealed no differences on chromosome 14 for *Prkcd* gene or the nearby *Tkt* gene (Figure 1F).

PKCδ has a unique expression profile among all the PKC family members. Since several members of the PKC family have previously been implicated in the regulation of insulin signaling in various tissues and cell models (14), we decided to perform a systematic gene expression analysis of all PKCs in order to establish whether any other PKC isoforms exhibited the unique hepatic expression pattern of PKCδ, i.e., a pattern characterized by (a) an inherited differential expression between B6 and 129 mice, (b) an induction of hepatic expression by HFD in the insulin resistance–prone B6 mice, (c) an absence of induction by HFD in insulin resistance–resistant 129 mice, and (d) a physical location near an SNP marker associated with the hyperinsulinemia observed in B6 versus 129 mice. Hepatic mRNA levels of conventional PKCs (α, β, and γ), novel PKCs (δ, ε, η, and θ) and atypical PKCs (ι/λ, ζ, and N1) were determined by quantitative real-time PCR (qPCR).

In 6-month-old chow-fed animals, B6 mice had significantly higher mRNA expression levels for PKCβ, -γ, -δ, -ε, -η, and -ι as compared with 129 mice (Figure 2A). Three of these PKCs (β, δ, η), as well as two others (θ and N1), were expressed at significantly greater levels in liver of B6 newborn mice compared with liver of 129 newborn mice, with PKCδ being the most significantly different (Figure 2B). Following HFD feeding, hepatic expression levels of PKCα, -γ, -δ, -ε, -η, -δ, and N1 were significantly increased in B6, but not 129, mice (Figure 2A). Interestingly, in insulin-resistant, genetically obese *ob/ob* mice, a slightly different set of PKCs including PKCα, -β, -δ, -η, and -ι/λ was induced in liver, clearly demonstrating differential regulation of expression among PKC family members in different states of obesity (Figure 2C). More importantly, in the HFD-treated 129 mice, we still observed a significant increase in PKCγ and -η hepatic expression, whereas PKCδ did not exhibit any increase in its hepatic expression in response to high-fat feeding (Figure 2A). Finally, we analyzed the chromosomal locations of all PKCs in the mouse genome and compared them to the chromosomal locations of previously identified SNP markers for QTLs linked to insulin resistance or obesity identified by in our genome-wide scan of an F_2 intercross between B6 and 129 mice subjected to HFD feeding (Table 1). Of the 10 chromosomal locations of the different PKC isoforms, only PKCδ was physically associated, i.e., within 2 Mb of an SNP marker (*D14Mit52*) that has been linked to hyperinsulinemia observed in B6 mice (6). Thus, among all the PKC family members, only *Prkcd* exhibited the unique characteristics that defined it as one of the major genes that contributed to the differential susceptibility to insulin resistance between B6 and 129 mice.

Table 1
Chromosomal location of PKC genes and GWAS SNP markers previously associated with differential hyperinsulinemia or hyperleptinemia between B6 and 129 mice

Symbol	PKC gene	Gene chromosomal location	GWAS SNP marker	Marker chromosomal location	Distance
θ	*Prkcq*	Chromosome 2: 11,093,740–11,222,853	None		
ι	*Prkci*	Chromosome 3: 30,894,669–30,951,663	*D3Mit127*	Chromosome 3: 142,848,413–142,848,587	111.9 Mb
ι	*Prkci*	Chromosome 3: 30,894,669–30,951,663	*D3Mit278*	Chromosome 3: 71,816,030–71,816,141	40.9 Mb
ζ	*Prkcz*	Chromosome 4: 154,634,238–154,735,470	None		
γ	*Prkcg*	Chromosome 7: 3,303,916–3,331,005	None		
β	*Prkcb*	Chromosome 7: 129,432,265–129,777,916	None		
N1	*Pkn1*	Chromosome 8: 86,193,661–86,223,078	None		
α	*Prkca*	Chromosome 11: 107,794,701–108,205,242	*D11Mit199*	Chromosome 11: 101,749,082–101,749,224	6.0 Mb
η	*Prkch*	Chromosome 12: 74,685,784–74,879,172	*D12Mit231*	Chromosome 12: 101,804,026–101,804,175	26.9 Mb
δ	*Prkcd*	Chromosome 14: 31,408,544–31,439,396	*D14Mit52*	Chromosome 14: 33,251,845–33,251,994	1.8 Mb
δ	*Prkcd*	Chromosome 14: 31,408,544–31,439,396	*D14Mit192*	Chromosome 14: 72,317,211–72,317,472	40.9 Mb
ε	*Prkce*	Chromosome 17: 86,567,125–87,057,259	None		

Hepatic PKCδ expression is influenced by obesity in mice and humans as well as genetic background between B6 and 129 mice. Although the difference in PKCδ expression could be observed between B6 and 129 mice prior to the onset of obesity, other states of obesity and insulin resistance are also associated with regulation of PKCδ. Thus, *Prkcd* expression in liver was also increased in *ob/ob* mice versus controls (1.0 ± 0.2 vs. 1.7 ± 0.2, $P < 0.05$) (Figure 2C), and this was not reversed by short-term infusion of insulin and/or leptin (Supplemental Figure 2A; supplemental material available online with this article; doi:10.1172/JCI46045DS1).

To study the possible association of hepatic PKCδ levels in humans with obesity and metabolic syndrome, we performed qPCR on mRNA taken from liver samples of 6 lean, 7 obese nondiabetic, and 11 obese type 2 diabetic subjects studied at the Joslin Diabetes Center (15). The clinical data on these groups are presented in Supplemental Table 1. In addition, BMI was greater than 2-fold higher in obese subjects, and subjects with obesity also had fasting hyperinsulinemia and hypertriglyceridemia. By definition, patients with diabetes were also hyperglycemic. qPCR analysis of the liver samples revealed a more than 2-fold increase in *PRKCD* mRNA levels in livers of obese nondiabetic subjects, as well as a tendency toward increased *PRKCD* in livers of obese diabetic patients when compared with lean subjects (7.1 ± 2.3 vs. 16.6 ± 3.5 and 11.9 ± 2.0, $P < 0.04$) (Figure 3A). While there was variability among the samples from obese diabetic patients, most likely related to heterogeneity in diabetes treatment and the poor glycemic control in some individuals, when we considered all diabetic and nondiabetic obese subjects, the increase in *PRKCD* expression was significant (7.1 ± 2.6 vs. 13.7 ± 1.8, $P < 0.04$). Repeat gene expression analysis for *PRKCD* and all other PKCs in the lean versus obese samples confirmed the increase in *PRKCD* (6.8 ± 0.7 vs. 12 ± 1, $P < 0.005$) and revealed a significant increase in *PRKCE* expression (5.6 ± 0.6 vs. 10 ± 1, $P < 0.03$) in livers of obese nondiabetic patients compared with lean controls (Figure 3B). More importantly, there was a significant correlation between BMI and hepatic *PRKCD* expression in human subjects, further linking obese states to high *PRKCD* expression levels in liver ($P < 0.035$) (Figure 3B). Expression of *PRKCB*, *PRKCH*, and *PRKCI/L* also showed trends toward increases, but these did not reach statistical significance ($P = 0.06$), possibly due to the small sample size (Figure 3B). To further explore this relationship, we compared mRNA levels for *PRKCD* and other PKCs using liver samples from 96 obese patients included in the study by Pihlajamaki et al. (16). These levels correlated with multiple physiological parameters including fasting insulin, glucose, age, circulating triglycerides, and homeostatic model assessment of insulin resistance (HOMA-IR) status. While there was a good deal of scatter in the data, there were positive correlations between *PRKCD* and fasting glycemia ($\rho = 0.262$, $P = 0.01$) (Figure 3D), as well as circulating triglycerides levels ($\rho = 0.207$, $P < 0.05$) (Figure 3E). None of the other novel PKCs (ε, η, and θ) showed any correlations with these parameters (Table 2).

Since obesity is associated with increased inflammation in fat, and B6 and 129 mice differ in the level of basal inflammation (17), we tested whether injection of bacterial LPS, which triggers a massive, generalized inflammatory response, would lead to changes in the expression of PKCδ. While B6 mice again had higher basal levels of *Prkcd* expression than 129 mice, no significant increase in *Prkcd* was observed in response to LPS treatment in either strain of mice (Supplemental Figure 3A). ER stress has been shown to be associated with insulin resistance (18), and several studies have suggested a possible association between ER stress and PKCδ (19, 20). However, induction of ER stress by tunicamycin injection also produced no change in PKCδ expression, despite a clear increase in expression of the chaperone protein Bip (Supplemental Figure 3B). Finally, neither hyperglycemia nor insulin itself appeared to directly regulate PKCδ expression, since mice with streptozotocin-induced (STZ-induced), insulin-deficient diabetes showed no alteration in *Prkcd* expression either in the untreated state or after treatment with insulin or phlorizin (PHZ) to normalize their blood glucose levels (Supplemental Figure 3, C and D). Thus, the genetically programmed difference between B6 and 129 mouse strains appears to be independent of levels of hyperglycemia, insulin, or leptin and independent of the states of inflammation or ER stress that may occur to different levels in these strains when subjected to HFD-induced obesity.

PKCδ-knockout mice display improved glucose tolerance and insulin sensitivity. To determine how the differences in PKCδ expression could contribute to the differences in insulin sensitivity and metabolic phenotype of B6 versus 129 mice, we studied three different mice models with alterations in PKCδ expression: (a) mice with global

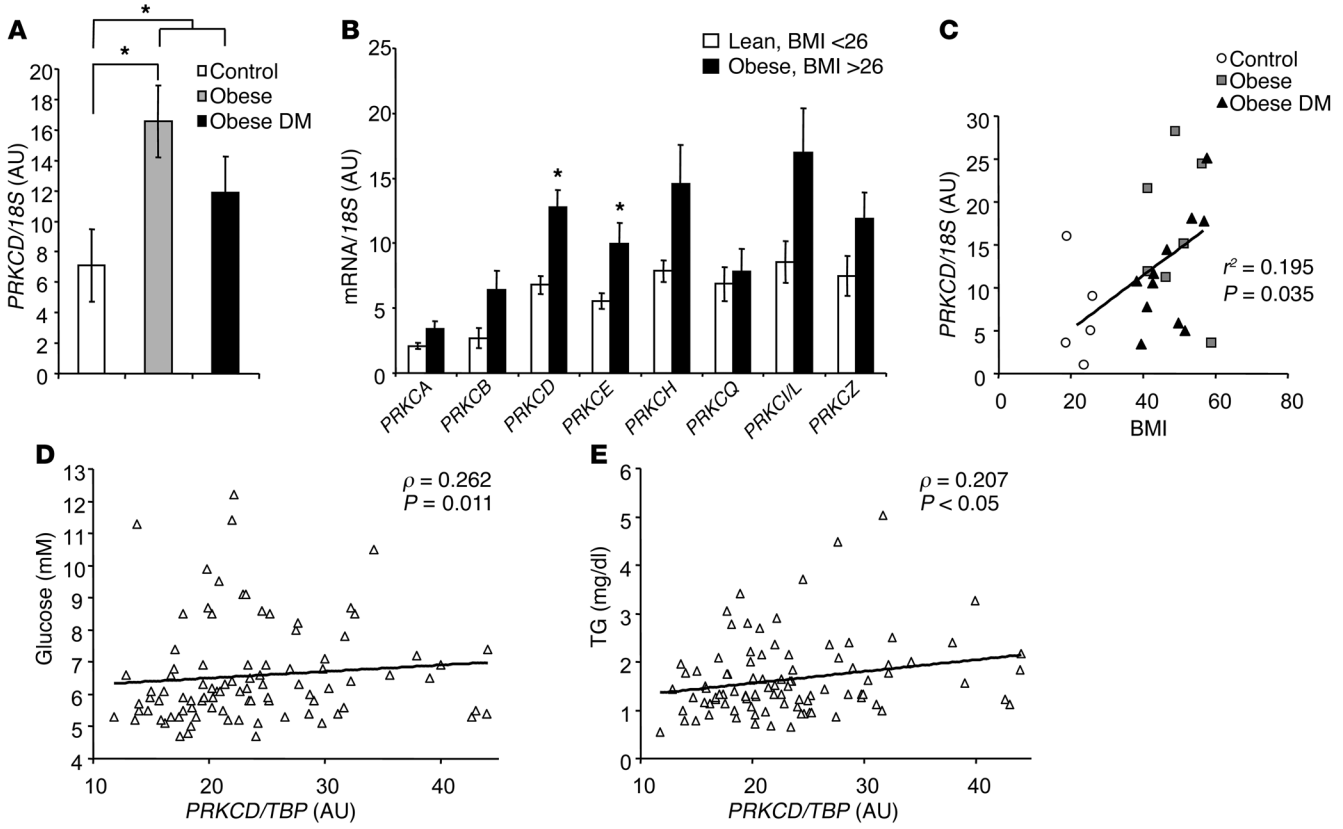

Figure 3

Hepatic expression of PKCδ is increased in obese subjects and correlates with fasting glucose and circulating triglycerides. Liver mRNA expression was measured by qPCR for (**A**) *PRKCD* in lean versus obese or obese diabetic subjects (n = 6–8–11 per group, *P < 0.04); and (**B**) all PKC isozymes in lean versus obese subjects (*P < 0.05). Correlations between hepatic *PRKCD* expression and (**C**) BMI, (**D**) fasting glucose, and (**E**) circulating triglycerides in human subjects.

inactivation of the *Prkcd* gene (PKCδKO) created by gene targeting; (b) mice with liver-specific inactivation of the *Prkcd* gene created using the Cre-lox system of conditional recombination; and (c) mice with overexpression of PKCδ in the liver achieved using adenovirus-mediated gene transfer. For our study, the PKCδKO mice previously described (21) were backcrossed onto a B6 genetic background for 14 generations. Although PKCδKO deficiency led to high rates of mortality when established on the B6 background, surviving PKCδ-deficient mice appeared generally healthy. On a regular chow diet at 20 weeks of age, PKCδKO mice had slightly lower body weights than their WT littermates (30 ± 0.7 and 35 ± 1 g, P < 0.05) (Figure 4A). Intraperitoneal glucose tolerance testing (GTT) revealed that PKCδKO mice had significantly better glucose tolerance than their control littermates (Figure 4B), with a 24% decrease in the AUC for glucose levels following the glucose challenge (Supplemental Figure 1A). Hyperinsulinemic-euglycemic clamp studies confirmed the increased whole body insulin sensitivity, with a striking 7-fold increase in the glucose infusion rates in PKCδKO compared with WT mice (25 ± 6 vs. 3.5 ± 0.5 mg/kg/min, P < 0.05) (Figure 4C), suggesting increased glucose uptake into muscle and/or fat. This increase in peripheral insulin sensitivity was accompanied by increased insulin sensitivity of the liver, with an increased ability of insulin to suppress hepatic glucose production (HGP). Thus, in the basal state, WT and PKCδKO mice had similar levels of HGP, but during the insulin clamp, PKCδKO displayed an 83% ± 6.9% inhibition of HGP versus a 63% ± 8.9% inhibition for the WT mice (Figure 4D). This difference in the ability of insulin to suppress gluconeogenesis was due to differences in insulin's ability to regulate gluconeogenic gene expression. Thus, the PKCδKO mice had a 33% decrease in phosphoenolpyruvate carboxykinase (*Pepck*), a 62% decrease in glucose-6-phospatase (*G6P*; also known as *G6pc*), and a 48% decrease fructose-1,6-bisphosphatase (*F1,6BP*; *Fbp1*) compared with controls (Figure 4G). PKCδ-null mice also had decreased expression of the key lipogenic transcription factors SREBP1c (*Srebf1*) (70%) and chREBP (*Mlxipl*) (79%), and this was associated with a major reduction in the expression of their transcriptional targets including the lipogenic enzymes fatty acid synthase (*FAS*; *Fasn*) (89%), acetyl-coA-carboxylase (*ACC*; *Acaca*) (88%), and stearoyl-CoA desaturase 1 (*Scd1*) (88%). Glucokinase (*Gck*), another transcriptional target of SREBP1c, also showed a major reduction (68%) in expression in PKCδ-deficient livers. This reduction in expression of lipogenic enzymes was accompanied by protection against age-related hepatosteatosis, as shown in histological analysis of liver sections from 12-month-old PKCδKO versus control mice (Figure 4E) and a 50% decrease in hepatic triglyceride content (Figure 4F).

PKCδ ablation also improved hepatic insulin signaling as assessed by Western blot analysis of liver extracts from mice taken during the hyperinsulinemic-euglycemic clamp. As shown in Figure 4H, PKCδKO mice had increased insulin stimulation of Akt phosphor-

Table 2
Spearman rank correlations between novel PKCs and characteristics of study subjects

	Age	Triglycerides	Glucose	Insulin	HOMA-IR
Prkcd/*Tbp*	–0.003	0.202[A]	0.262[A]	0.005	0.071
Prkce/*Tbp*	–0.098	–0.054	–0.090	0.203	0.163
Prkch/*Tbp*	–0.070	0.108	0.165	–0.023	0.050
Prkcq/*Tbp*	0.093	0.189	0.136	–0.030	0.018
n	96	95	93	91	88

[A]Significant correlation ($P < 0.05$).

ylation and phosphorylation of the p42 and p44 MAPKs. PKCδKO mice also had increased insulin-stimulated phosphorylation of p70S6 kinase (p70S6K) on Thr421/Ser424, a site known to inhibit p70S6K activity (22, 23). As a consequence, there was a decrease in the phosphorylation of IRS-1 on Ser307 to almost undetectable levels in PKCδKO mice (Figure 4H). Ser307 is a known site of IRS-1 phosphorylation by p70S6K phosphorylation, which leads to inhibition of insulin action (23). Taken together, these results demonstrate that whole body deletion of PKCδ improves insulin sensitivity in both liver and peripheral tissues and improves insulin action at the level of the liver.

Liver-specific overexpression of PKCδ leads to metabolic syndrome symptoms. To further define the role of increased PKCδ in the liver, we created B6 mice in which we induced overexpression of PKCδ in liver by adenoviral delivery of PKCδ cDNA. This resulted in an 8-fold increase in the levels of PKCδ in liver as determined by Western blot analysis. On intraperitoneal glucose challenge, mice overexpressing PKCδ were glucose intolerant in comparison with GFP-overexpressing control mice created in parallel, with a 33% increase in AUC of the GTT (Figure 5A and Supplemental Figure 1B). Interestingly, when we overexpressed PKCδ in liver of 129 mice, we also observed a subsequent diminution of their glucose tolerance, which became more similar to that of the glucose-intolerant B6 control mice (Supplemental Figure 2B). In contrast to the decreased gluconeogenesis in PKCδKO mice, mice with increased levels of hepatic PKCδ had increased gluconeogenesis as demonstrated by an exaggerated response to a pyruvate tolerance test (PTT), with a 38% increase in AUC compared with control mice (Figure 5B and Supplemental Figure 1D). This also resulted in an approximately 20% increase in plasma glucose in both the fasted and fed states (compare 0 time points in Figure 4, A–C, respectively). Although basal glucose levels were increased, there was no difference in the insulin-mediated reduction of glucose levels during an intraperitoneal insulin tolerance test (ITT), suggesting that there was no difference in insulin sensitivity in muscle between the mice overexpressing PKCδ in liver and the controls (Figure 5C).

In addition to its effect on glucose metabolism, overexpression of PKCδ in liver resulted in a significant increase in hepatosteatosis, which was easily observed in H&E-stained histological sections of liver (Figure 5E). This correlated with a 33% increase in hepatic triglyceride content in mice overexpressing PKCδ compared with controls (Figure 5F). In 2-hour-fasted animals, overexpression of PKCδ in the liver also resulted in mild hyperglycemia (85 ± 3.6 vs. 69 ± 3.4 mg/dl in controls), hyperinsulinemia (0.33 ± 0.04 vs. 0.18 ± 0.03 ng/ml), and hypertriglyceridemia (101 ± 3 vs. 66 ± 4 mg/dl) (Figure 5, D–F). Thus, overexpression of PKCδ in liver reproduced the differential glucose tolerance differentiating B6 from 129 mice as well as many of the signs of the metabolic syndrome, even in lean mice on regular chow diet.

PKCδ overexpression alters hepatic insulin signaling. The physiological alterations induced by PKCδ overexpression were associated with hepatic insulin resistance at the level of the insulin signaling pathway. While PKCδ overexpression did not alter tyrosine phosphorylation of the insulin receptor itself (data not shown), overexpression of PKCδ resulted in a significant decrease in insulin-stimulated phosphorylation of IRS-1 on Tyr612 and decreased phosphorylation of Akt and glycogen synthase kinase 3 (GSK3) on Ser473 and Ser9, respectively. As opposed to what had been observed in PKCδKO mice, p70S6K phosphorylation on Thr389 in response to insulin was greatly enhanced by PKCδ overexpression, and this correlated with the increased phosphorylation of IRS-1 on Ser307 (Figure 6A). As a consequence of the repression of insulin signaling, Foxo1 nuclear localization was enhanced about 2-fold in livers of mice overexpressing PKCδ, as demonstrated by Western blotting of nuclear extracts (Figure 6D). Consistent with the role of Foxo1 as a regulator of hepatic gluconeogenesis (24), mice overexpressing PKCδ had 1.2- to 2.5-fold increases in the levels of mRNA for the gluconeogenic enzymes *Pepck*, *G6pc*, and *Fbp1* (Figure 6B).

Overexpression of PKCδ also increased the levels of SREBP1c 2-fold at both mRNA and protein levels (Figure 6, B and C), as well as *Mlxipl* 2-fold at the mRNA level. This was accompanied by a 2-fold increase in the expression of the three key lipogenic enzymes *Fasn*, *Acaca*, and *Scd1*, as well as *Gck*, all transcriptional targets of *Srebf1* (Figure 6B). Thus, increasing the expression of PKCδ by only a few fold was sufficient to induce a significant liver insulin resistance and stimulate basal hepatic lipogenesis.

Liver-specific reduction of PKCδ restores glucose tolerance and insulin signaling in HFD-induced diabetic animals. To determine whether decreasing PKCδ specifically in the liver could improve the hepatic insulin sensitivity in obese diabetic mice, we created a liver-specific PKCδ-knockout mouse. To this end, exon 2 of the *Prkcd* gene was flanked with two loxP sites and introduced in mice by homologous recombination. Loss of exon 2 of the floxed *Prkcd* gene results in a deletion and frameshifts the PKCδ transcript, leading to the production of a truncated, inactive PKCδ protein (Supplemental Figure 2C). Intravenous administration of an adenoviral vector containing a Cre recombinase expression cassette resulted in recombination of the *Prkcd* transgene in liver. At the dose of adenovirus used, 5 days after injection, there was a reproducible 40% reduction in PKCδ mRNA and protein compared with control mice injected with empty adenoviral vector (Figure 7A).

To assess the consequences of reduced levels of PKCδ on hepatic insulin resistance, we injected empty or Cre recombinase–expressing adenoviruses into 3-month-old PKCδ-floxed mice that had previously been subjected to 10 weeks of either a HFD (60% fat by calories) or a regular chow diet (23% fat by calories). Five days after adenovirus injection, there were no differences in body weight between floxed mice and mice with liver-specific knockdown of PKCδ on either the chow diet or HFD (data not shown). As expected, however, mice that had been on HFD for 10 weeks were glucose intolerant compared with the chow diet–fed control animals. Furthermore, while the modest reduction of PKCδ had no effects on glucose tolerance in lean mice, liver-specific reduction of PKCδ in the HFD obese mice was sufficient to significantly improve the glucose tolerance as compared with the

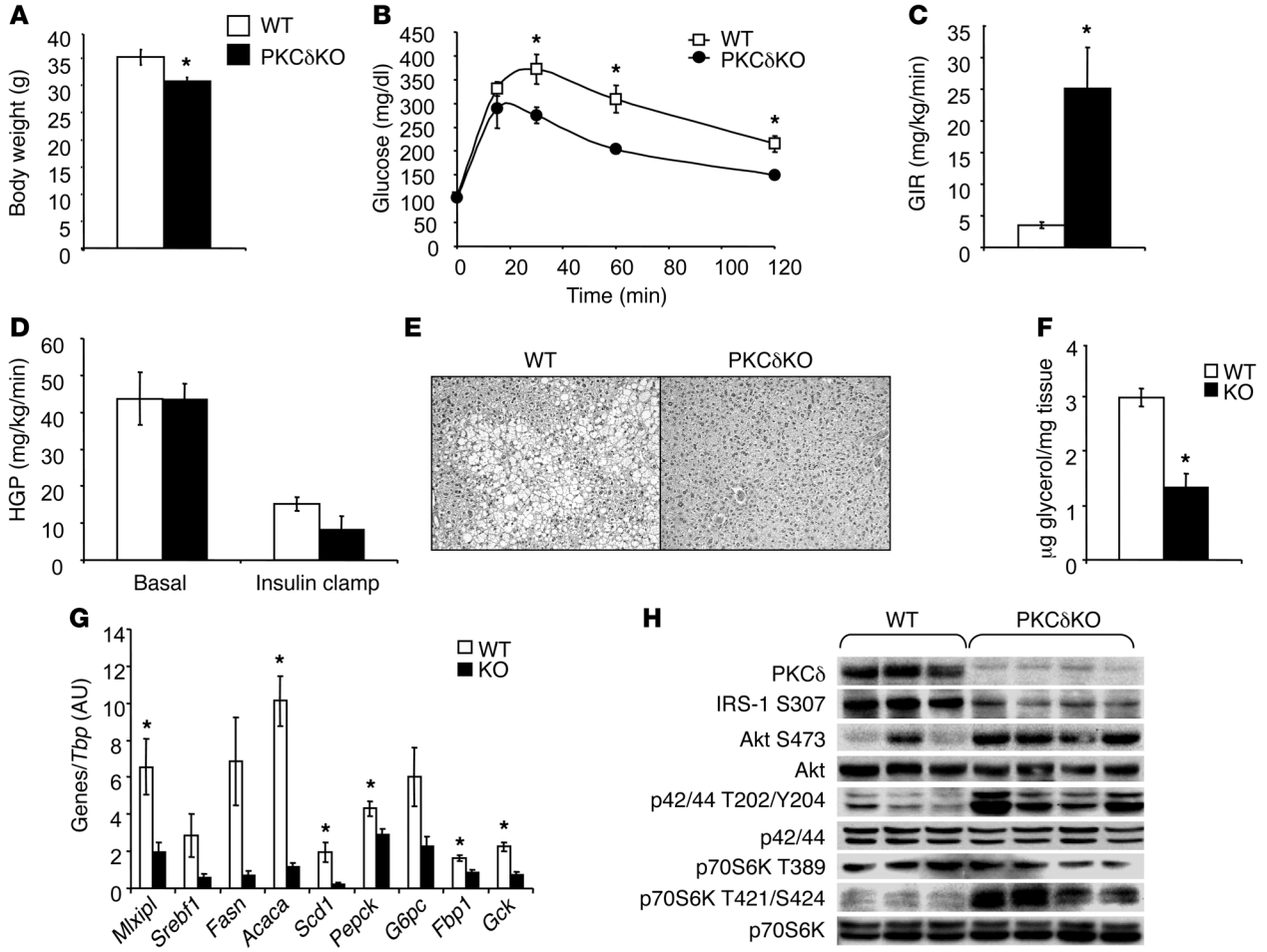

Figure 4

PKCδKO mice display improved glucose tolerance and hepatic insulin sensitivity. (**A**) Body weight of WT versus PKCδKO mice ($n = 8$ per group, $^*P < 0.02$). (**B**) GTT of WT versus PKCδKO mice ($n = 5$ per group, $^*P < 0.03$). (**C**) Glucose infusion rate (GIR) and (**D**) HGP during euglycemic-hyperinsulinemic clamps of WT versus PKCδKO mice ($n = 4$ per group, $^*P < 0.05$). (**E**) H&E-stained sections of liver from 1-year-old WT and PKCδ KO mice (original magnification, ×200). (**F**) Triglyceride levels in liver of WT and PKCδKO mice ($n = 4$ per group, $^*P < 0.05$). (**G**) qPCR analysis of mRNA for gluconeogenic and lipogenic genes in liver at the end of the euglycemic-hyperinsulinemic clamp in control versus PKCδKO mice ($n = 4$ per group, $^*P < 0.04$). (**H**) Western blot analysis of proteins in the insulin signaling pathway in liver at the end of the euglycemic-hyperinsulinemic clamp. Each lane represents an individual animal.

obese empty adenovirus–treated controls, as demonstrated by a significant 20%–25% reduction in the AUC for glucose (Figure 7B and Supplemental Figure 1E).

This improvement in metabolism was secondary to an improvement in insulin signaling. Thus, in the HFD obese control mice, insulin signaling was markedly blunted, with no detectable increase in Akt phosphorylation following insulin stimulation (Figure 7C). This was due to high levels of inhibitory phosphorylation of IRS-1 on Ser307, which was secondary to high levels of p70S6K activation as indicated by p70S6K phosphorylation. Reducing PKCδ reversed many of these changes. Thus, there was a reversal of p70S6K phosphorylation/activation, leading to a reduction in IRS-1 Ser307 phosphorylation levels and a rescue of Akt/GSK3 phosphorylation/activation by insulin (Figure 7C). Parallel to this improvement in insulin signaling, we also observed reduction in expression of gluconeogenic genes such as *G6pc* and *Fbp1* (Figure 7D). Despite the improvement in glucose tolerance, however, this short-term reduction in PKCδ did not improve the hepatosteatosis present in HFD obese mice as assessed by histological examination of liver sections (Supplemental Figure 2E) and measurement of liver triglyceride content (Supplemental Figure 2F). Likewise, there was no change in gene expression levels for the lipogenic genes *Srebf1*, *Mlxipl*, *Fasn*, *Acaca*, or *Scd1* (Figure 7D and data not shown). Finally, we did not observe any modulation of the hyperinsulinemia, hypertriglyceridemia, or the high levels of free fatty acids induced by HFD (Supplemental Figure 2D). Therefore, a short-term reduction of hepatic PKCδ was sufficient to rescue glucose tolerance and insulin signaling in the liver of HFD-fed mice, but not sufficient to reverse the secondary hyperinsulinemia or the lipid abnormalities in these mice.

Discussion

T2D and the related metabolic syndrome are the results of interaction between disease risk genes and environmental promoters. This role of gene-environment interaction in the development of metabolic disease is also observed in mice of different strains carrying in their background different disease risk genes. For example,

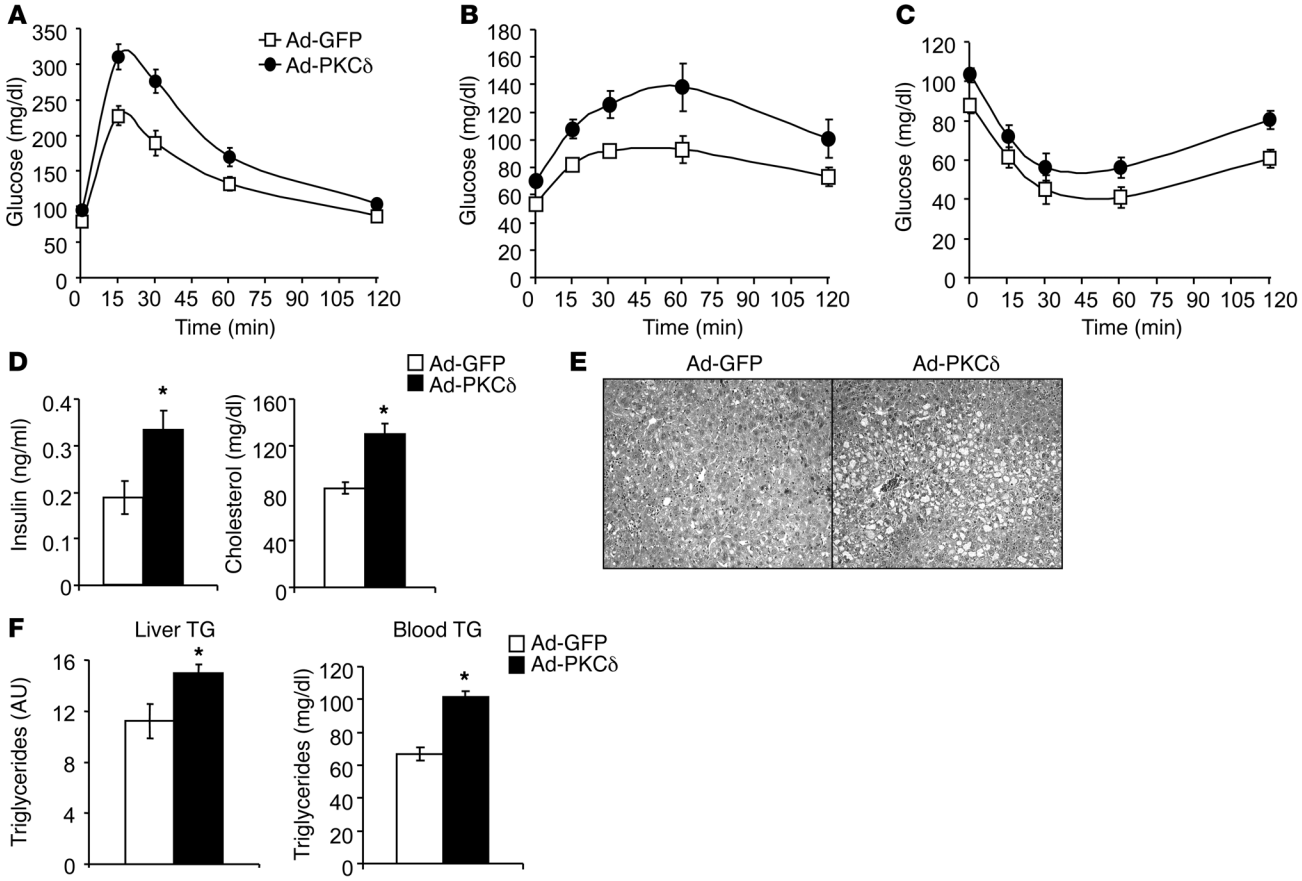

Figure 5

Mice with liver-specific overexpression of PKCδ develop features of the metabolic syndrome. (**A**) GTT in mice overexpressing GFP or PKCδ in the liver (n = 13 per group). (**B**) PTT in mice overexpressing GFP or PKCδ in the liver (n = 9 per group). (**C**) ITT in mice overexpressing GFP or PKCδ in the liver (n = 19 per group). (**D**) Serum insulin and cholesterol levels in mice overexpressing GFP or PKCδ in the liver. (**E**) Histological pictures of H&E-stained liver sections from mice overexpressing GFP or PKCδ in the liver (original magnification, ×200). (**F**) Triglyceride levels in blood and liver of 2-hour-fasted mice overexpressing GFP or PKCδ in the liver (n = 8 per group, $^*P < 0.01$).

B6 mice are prone to becoming obese as they age on either high- or low-fat diet, whereas 129 mice are relatively resistant to obesity on either diet. Furthermore, on both the low- and high-fat diet, B6 mice have higher insulin levels and inferior glucose and insulin tolerance compared with 129 mice, indicating that B6 mice develop more insulin resistance than 129 mice. This difference in susceptibility to insulin resistance is also apparent when B6 and 129 mice are subjected to a genetic insulin resistance challenge. Thus, B6 mice that are double heterozygous for knockout of the insulin receptor and *Irs1* genes exhibit marked hyperinsulinemia and massive islet hyperplasia and develop early hyperglycemia, with more than 85% of mice becoming overtly diabetic by 6 months. By contrast, 129 mice with the same double heterozygous deletions show very mild hyperinsulinemia and minimal islet hyperplasia, and less than 2% of mice develop diabetes by the age of 6 months. The severe diabetes and insulin resistance in B6 double heterozygous mice versus the almost complete lack of disease in the 129 mice carrying the same mutations indicate the strength of the genetic modifiers between these strains. Identifying the specific background genes that modify insulin resistance is therefore an important challenge and could provide novel targets for therapy and prevention of T2D.

Genome-wide scanning of the F_2 intercross between B6 and 129 mice identified 8 QTLs on 6 different chromosomes linked to these different responses to HFD and the double heterozygous knockout (6). The strongest QTL linked with hyperinsulinemia/insulin resistance is on chromosome 14. Consistent with an important genetic determinant at this locus of insulin resistance, mice homozygous for the B6 allele in this region have 6-fold-higher insulin levels than mice homozygous for the 129 allele when placed on HFD, and mice heterozygous for B6 and 129 alleles had intermediate levels. Several candidate genes for insulin resistance are present in this region, the most prominent of which is *Prkcd*.

In the present study, using 3 different in vivo models, we demonstrate that PKCδ is a major regulator of insulin resistance and is at least one of the major genetic modifiers of the diabetic risk between these two strains of mice. PKCδ also acts as a major modulator of the risk of development of hepatic steatosis between these strains of mice. We establish the importance of PKCδ not only by finding differences in expression levels, but also by showing that PKCδ can regulate whole body and hepatic insulin sensitivity and hepatic lipid accumulation through liver-specific overexpression, whole body knockout, and liver-specific reduction in PKCδ. Importantly, PKCδ expression is also increased in

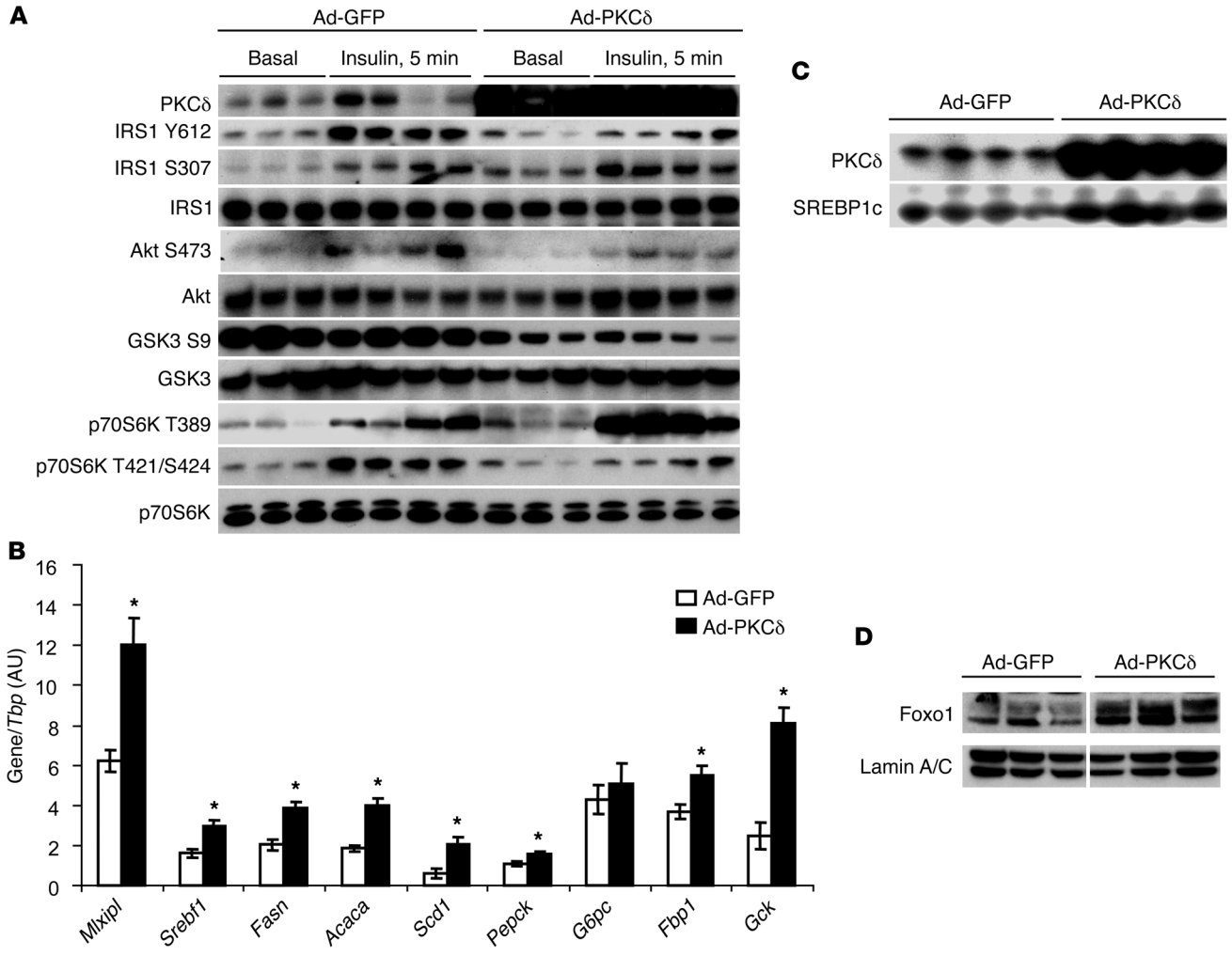

Figure 6

High hepatic PKCδ expression levels lead to hepatic insulin resistance. (**A**) Western blot analysis of insulin signaling pathway in liver of mice overexpressing GFP or PKCδ in the liver 5 minutes after intraperitoneal injection of insulin or vehicle as described in Methods. (**B**) qPCR analysis in liver overexpressing GFP or PKCδ of lipogenic gene expression ($n = 6$ per group, $^{**}P < 0.01$) and gluconeogenic gene expression ($n = 6$ per group, $^{*}P < 0.05$). Results are normalized to *Tbp*. (**C**) Western blot analysis of PKCδ and SREBP1c expression in liver overexpressing GFP or PKCδ. (**D**) Western blot analysis of Foxo1 and lamin A/C expression in nuclear extracts of liver overexpressing GFP or PKCδ. Lanes in **D** were run on the same gel but were noncontiguous.

livers of obese and obese type 2 diabetic subjects and in obese subjects correlates with hyperglycemia and hypertriglyceridemia, suggesting that this enzyme also plays a role in the development of human metabolic syndrome.

All major insulin-responsive tissues (skeletal muscle, adipose tissue, and liver), like most tissues of the body, express multiple isoforms of each of the 3 PKC classes (25). Through the use of transgenic and knockout approaches, several members of the PKC family have been implicated in insulin action, the development of insulin resistance, and the regulation of metabolism. In mice with deletion of the *Prkca* gene, insulin signaling through IRS-1–dependent activation of PI3K and of its downstream processes including glucose transport are enhanced in muscle and adipose tissue (26). Likewise, knockout of the *Prkcb1* gene mildly enhances overall glucose homeostasis in vivo (27). Deletion of PKCε improves glucose-stimulated insulin secretion, reduces insulin clearance, and protects against hepatic insulin resistance, whereas muscle-specific inactivation of PKCι/λ has been shown to impair glucose transport (28). Excessive activation of the atypical PKCζ has been shown to activate SREBP1c and NF-κB and contribute to hyperlipidemia and systemic insulin resistance (29), and we have also demonstrated the existence of divergent regulation of hepatic glucose and lipid metabolism dependent on PI3K and PKCι/ζ (30). Studies on PKCθ inactivation have reported conflicting effects on HFD-induced insulin resistance (31, 32).

In the current study, we demonstrate that PKCδ has unique characteristics among the PKC family members that define it as a major modifier of the diabetic risk between B6 and 129 mice, as well as in obese and diabetic humans. There are at least two aspects in PKCδ expression that differentiate B6 mice from 129 mice. First, expression analysis performed on liver, muscle, and adipose tissue of B6 and 129 mice on normal chow reveals higher expression of PKCδ in all tissues

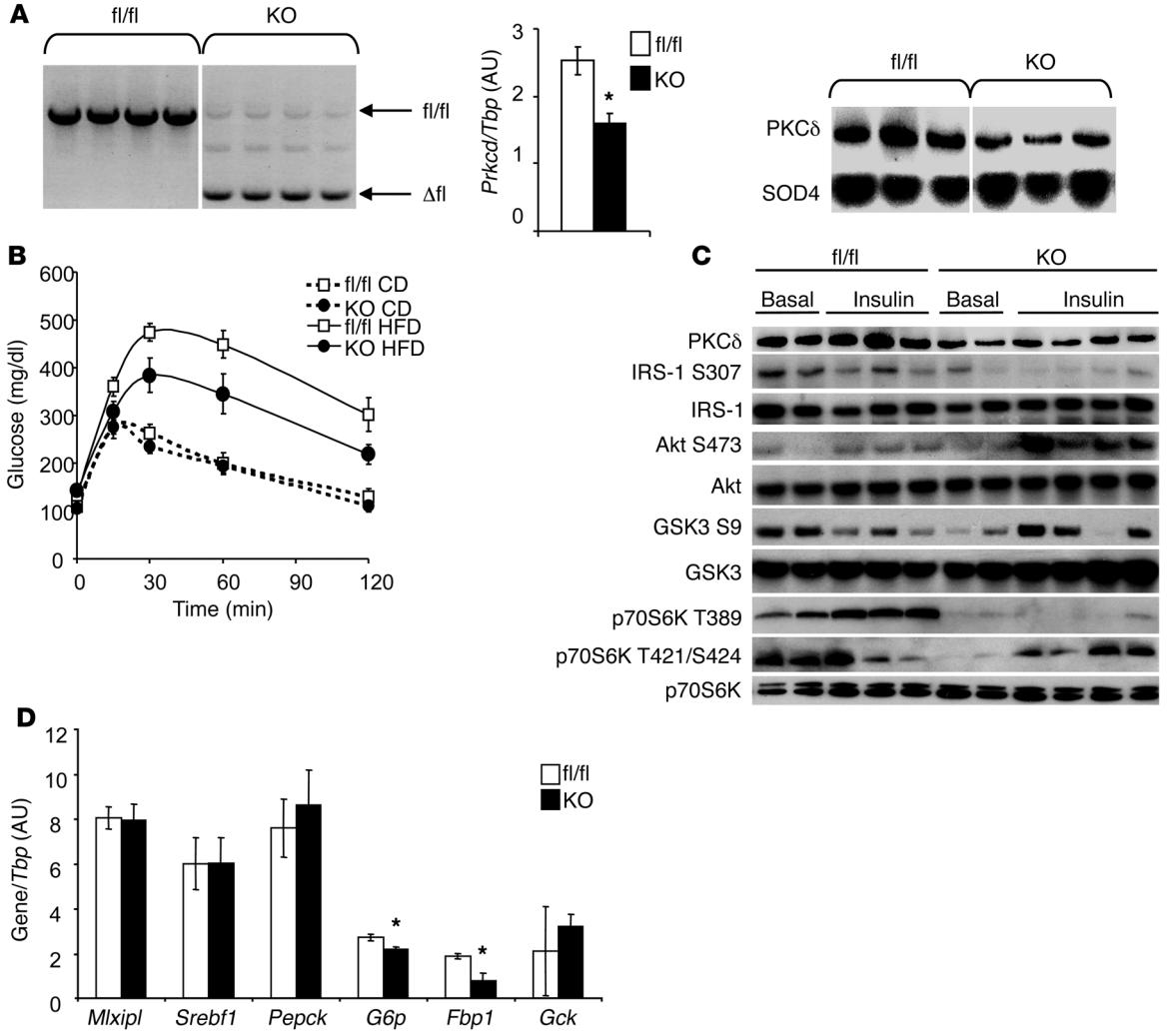

Figure 7

Liver-specific reduction of PKCδ expression improves HFD-induced hepatic insulin resistance. (**A**) Validation of effective DNA recombination by PCR analysis of genomic DNA, qPCR measurement of *Prkcd* mRNA expression ($n = 6$ per group, $^*P < 0.005$), and Western blot analysis of PKCδ protein in livers of PKCδ-floxed mice after administration of empty or Cre recombinase–expressing adenovirus. (**B**) GTT of PKCδ-floxed mice injected with empty (white squares) or Cre recombinase–expressing adenovirus (black circles) following 10 weeks of CD (dashed lines) or HFD (plain lines) feeding ($n = 6$ per group). (**C**) Western blot analysis of insulin signaling pathway in liver of PKCδ-floxed mice injected with empty or Cre recombinase–expressing adenovirus following 10 weeks of CD or HFD feeding and 5 minutes after injection of insulin or vehicle as described in Methods. (**D**) qPCR analysis in liver overexpressing GFP or PKCδ of lipogenic and gluconeogenic gene expression in liver of PKCδ-floxed mice injected with empty or Cre recombinase–expressing adenovirus following 10 weeks of HFD ($n = 14$ per group, $^*P < 0.05$). Results are normalized to *Tbp*.

from B6 compared with 129 mice at 6 months of age (6). Indeed, PKCδ expression in liver was higher in B6 mice compared with 129 mice at 6 weeks, an age when they are metabolically indistinguishable, as well as at birth, pointing to a genetically programmed difference between these strains as opposed to a change secondary to diet, obesity, or metabolic derangement. Second, upon exposure to HFD, expression of PKCδ in the liver was further increased in B6 mice, but not increased at all in 129 mice, pointing to a genetic impact on the control of the environmental mediated regulation of PKCδ expression in the liver of B6 and 129 mice on top of the basal genetic difference. The exact cause for the difference in PKCδ expression remains unclear, but it is not due to differences in gene copy number or to difference in the sequence of the coding region of the gene. Further genetic analyses are underway to identify possible genetic differences in the promoter region of *Prkcd* and/or the methylation state of a large CpG island present in the first intron of the *Prkcd* gene. Whether humans also exhibit genetically programmed differences in regulation of PKCδ expression that might contribute to genetic risk of diabetes will also require further study, but obese humans with or without T2D clearly show increased expression of PKCδ in liver. Interestingly, a major locus associated with metabolic syndrome phenotypes has been identified in a region on human chromosome 3p that includes the *Prkcd* locus (33).

Recently, several studies have indicated the importance of PKCδ in tissues involved in diabetes pathogenesis, including muscle, pancreas, and vascular tissues. PKCδ has been shown to modify

glucose uptake in myotubes (34), lipogenesis in liver (12), development of ER stress in hepatoma cells (19), and development of vascular changes in the retina (35). A role of PKCδ in the regulation of insulin secretion has also been reported in two studies using PKCδ transgenic mouse models (36, 37), but the results of the latter were conflicting as to the direction of change. Our findings indicate that PKCδ is a significant modifier of insulin sensitivity. Indeed, in mice on a normal chow diet, whole body PKCδ-null mice exhibited an impressive 7-fold increase in glucose infusion rate during a euglycemic-hyperinsulinemic clamp, associated with increased insulin sensitivity in liver to insulin inhibition of glucose production. Such differences in glucose infusion rates could not be solely due to a reduction in HGP, and suggest an improvement in insulin sensitivity in muscle and/or adipose tissue, where most of the glucose uptake occurs. In ongoing experiments, the contribution of each of these tissues to the observed phenotype will be assessed by the use of mouse models with muscle-specific and adipose tissue–specific deletions of the *Prkcd* gene.

In the normal liver, insulin suppresses Foxo1 and gluconeogenesis while stimulating SREBP1c and lipogenesis (38). In T2D, a state of insulin resistance, insulin is unable to suppress gluconeogenesis normally, but SREBP1c and lipogenesis are elevated (39). How SREBP1c is induced in T2D remains an important but unanswered question (40). One possibility is that the specific branch of the insulin signaling cascade that activates lipogenesis remains sensitive to insulin, even as the branch regulating gluconeogenesis becomes resistant. Recent evidence has shown that insulin stimulates SREBP1c via mTORC1 (41), raising the possibility that the combination of hyperglycemia and hypertriglyceridemia in T2D is due to a failure to suppress Foxo1 coupled with increased mTORC1 signaling.

Our data suggest that PKCδ may be a key player in the development of T2D. We find that both genetic and environmental insults can induce PKCδ, and this in turn produces defects in signaling through Foxo1, resulting in increased levels of gluconeogenic genes and hyperglycemia. The improvement in insulin sensitivity in liver of PKCδKO mice is linked to an improvement in the early steps of insulin signaling, in particular an increase in tyrosine phosphorylation of IRS-1 leading to increased signaling down the PI3K/Akt pathway. This improvement is associated with a decrease in the phosphorylation of IRS-1 on Ser307, one of the end points of a signaling cascade attempting to reestablish insulin sensitivity in insulin-resistant liver (42). The effect of PKCδ appears to be mediated through p70S6K, which shows enhanced phosphorylation/activation in states where PKCδ levels are high and decreased phosphorylation/activation in states where PKCδ levels are low. On the other hand, PKCδ promotes signaling to SREBP1c. This appears to occur via mTORC1 as indicated by activation of the mTORC1 target p70S6K.

PKCδ may also affect insulin sensitivity by regulation of inflammation. For example, in hepatocytes in vitro, PKCδ serves as an intermediate in response to TNF-α activation of NF-κB and the ER stress response (19). PKCδ has also been shown to play a role in production of ROS in adipocytes from HFD-treated animals, and this could further contribute to insulin resistance and risk of T2D (43, 44). PKCδ could also participate in the development of inflammation in adipose tissue, as PKCδ activation in mesenteric fat has been shown to lead to secretion of the proinflammatory cytokine IL-6 by adipocytes (45). In this study, we observed that PKCδ-deficient mice exhibit protection against adipose tissue inflammation associated with insulin resistance (Supplemental Figure 3E). Moreover, using Gene Network Enrichment Analysis (GNEA) to integrate gene expression data for different tissues from B6 versus 129 mice of varying ages and dietary conditions, we have recently shown significant differences in expression of immune system–related genes in the adipose tissue of B6 versus 129 mice, even prior to the onset of obesity (17). This results in elevated expression of inflammatory markers in B6 as compared with 129 mice and increased infiltration of adipose tissue with macrophages and T cells. As mice age, or when they are subjected to HFD, the disparity in the inflammatory status of the adipose tissue becomes even more pronounced. Thus, the differences in the repertoire of inflammatory cells in the fat tissue are associated with the predisposition to metabolic diseases. This study together with our present findings demonstrate how PKCδ can serve as a major mediator of insulin resistance, as well as the deleterious effects of inflammation on insulin signaling, in liver and other insulin-sensitive tissues.

Some studies have also reported that PKCδ may be a target of or play a role in insulin action. In L6 myotubes, insulin is capable of regulating PKCδ protein levels through both transcriptional (46) and post-transcriptional (47) mechanisms. Insulin also increases the amount of PKCδ within the nuclear fraction of L6 myotubes. Finally, some studies suggest that insulin can induce PKCδ activation through Src tyrosine kinase, and that PKCδ plays a positive role in insulin-stimulated glucose transport (34, 48–50). Whatever the exact mechanisms involved in these potentially positive roles of PKCδ, our results indicate that the major effect of high PKCδ is inhibition of insulin action in vivo and that deletion of PKCδ will improve insulin action and steatosis in liver and lead to an overall improvement in glucose tolerance and increase in whole body insulin sensitivity, as demonstrated by the euglycemic-hyperinsulinemic clamp. These finding are supported by a recent study showing that inhibition of PKCδ in mice under HFD conditions improves their glucose tolerance (12).

In addition to PKCδ, several other PKCs are present and differentially regulated in liver in response to stimuli such as HFD and therefore may also participate in the regulation of hepatic metabolism and insulin sensitivity. For example, PKCα is induced by HFD treatment and can act to inhibit insulin signaling via phosphorylation of IRS-1 (51). PKCε has also been shown to play a role in hepatic insulin resistance (52), and our results show that PKCε expression is also enhanced in liver of HFD-treated animals and/or *ob/ob* mice. Indeed, the whole subclass of novel PKC isozymes is induced by most environmental stressors associated with the development of hepatosteatosis and hepatic insulin resistance. Thus, one may need to develop agents that target multiple members of this group if one is to use these as targets to treat the hepatic dysregulation associated with the metabolic syndrome.

However, PKCδ appears to play a unique role as a modifier of insulin sensitivity. First, its expression is genetically programmed, allowing PKCδ to serve as an inherited modifier of insulin sensitivity in mice. Second, regulation of PKCδ expression is also genetically controlled, increasing in insulin resistance–prone, but not insulin resistance–resistant, strains of mice subjected to HFD. Third, the *PRKCD* gene is located in a region of human chromosome 3 previously linked to the metabolic syndrome, and PKCδ expression is upregulated in human obese and obese diabetic subjects to an extent similar to that seen in obesity- and insulin

resistance–prone strains of mice. Finally, relatively moderate differences in expression of PKCδ can change the risk for development of whole body and liver insulin resistance and the risk for development of hepatic steatosis. Thus, PKCδ represents a strong candidate for pharmaceutical treatment of insulin resistance, T2D, and the metabolic syndrome, as well as their associated complications such as hepatic steatosis.

Methods

Generation of Prkcd loxP/loxP mice. Lambda phage clones containing the murine *Prkcd* gene were isolated from a 129 mouse ES cell library, and a targeting vector containing approximately 9 kb in the two homology regions (Supplemental Figure 2C) was created and electroporated into E14/1 mouse ES cells. Stably transfected cells were isolated by selection with G418 (350 μg/ml; Gibco, Invitrogen), and clones were screened for the desired homologous recombination event. A 1.8-kb EcoRI/HindIII fragment was used as an external probe for Southern blot analysis of DNA digested with EcoRI (data not shown).

ES cell clones were injected into B6 mouse blastocysts, which were then transferred to pseudopregnant B6 female mice. Chimeric animals were screened for presence of the recombinant floxed allele by PCR using primers flanking the first and third loxP sites. Chimeric males were mated to B6 females that carried a Cre transgene under the control of the adenovirus EIIa promoter (The Jackson Laboratory), which targets expression of Cre recombinase to the early mouse embryo prior to implantation in the uterine wall. A mosaic pattern of expression is commonly observed, with Cre-mediated recombination occurring in a wide range of tissues, including the germ cells that transmit the genetic alteration to progeny. Progeny were screened by PCR to select *Prkcd* loxP/+ offspring containing two loxP site surrounding exon 2 and no Neo cassette. Offspring were analyzed by PCR of tail DNA to identify the *Prkcd* loxP/+ heterozygote mice. Heterozygotes were mated to generate homozygous *Prkcd* loxP/loxP mice. The *Prkcd* loxP/loxP mice were backcrossed for 14 generations with B6 to obtain a homogeneous B6 background.

Mice, diets, and adenoviral treatments. B6 male mice were obtained from The Jackson Laboratory; 129 male mice were obtained from Taconic. Mice were maintained on a 12-hour light/12-hour dark cycle with ad libitum access to tap water and standard chow diet containing 21% calories from fat, 22% protein, and 57% carbohydrates (PharmaServ). For some studies, 6-week-old mice were subjected to a low-fat diet — 14% of calories from fat, 25% from protein, and 61% from carbohydrates (Taconic) — or a HFD — 55% from fat, 21% protein, and 24% carbohydrates (Harlan Teklad) — for 18 weeks prior to sacrifice. Adenoviruses encoding PKCδ or GFP as control were prepared as previously described (53) and injected at a dose of 5×10^8 PFU/g body weight into the tail vein 5–10 days prior to sacrifice. Adenoviruses encoding Cre recombinase were purchased from the Gene Transfer Vector Core, University of Iowa. All protocols for animal use were reviewed and approved by the Animal Care Committee of the Joslin Diabetes Center and were in accordance with NIH guidelines.

Joslin study subjects. Individuals from 24 to 64 years of age undergoing elective surgery for obesity or gallstones participated in the study. Human studies were performed in accordance with the Declaration of Helsinki and were approved by institutional review boards of the Joslin Diabetes Center and Beth Israel Deaconess Medical Center. Samples included 6 control subjects, 7 obese subjects (BMI >30), and 11 obese patients diagnosed with diabetes. A more detailed description of the study subjects used in the qPCR experiments and their metabolic parameters is provided in Supplemental Table 1 and ref. 15.

Kuopio obesity surgery study. Ninety-six consecutive subjects (32 men, 64 women, age 47.1 ± 9.1 years, BMI 45.2 ± 6.3 kg/m^2) from an ongoing study including all subjects undergoing bariatric surgery at Kuopio University Hospital were included (16). Every participant had a 1-day visit including an interview and evaluation of cardiovascular risk factors. Fasting blood samples were drawn after 12 hours. Liver biopsy samples were taken at the time of bariatric surgery. The study was approved by the Ethics Committee of the Northern Savo Central Hospital Region, and it was in accordance with the Declaration of Helsinki.

All subjects provided informed consent prior to their participation in the study.

Mouse metabolic studies. For GTTs, blood samples were obtained at 0, 15, 30, 60, and 120 minutes after intraperitoneal injection of 2 g/kg dextrose. ITTs were performed by injecting 1 U/kg regular insulin (Novo Nordisk) intraperitoneally, followed by blood collection at 0, 15, 30, and 60 minutes. The pyruvate challenge was performed by injecting 2 g/kg pyruvate (Sigma-Aldrich) intraperitoneally, with blood glucose measured at 0, 15, 30, and 60 minutes. Blood glucose values were determined using a One Touch II glucose monitor (Lifescan Inc.).

Hyperinsulinemic-euglycemic clamp experiments. The jugular vein of mice was cannulated, and after a 1 week of recovery period and a 4-hour fast, a hyperinsulinemic-euglycemic clamp was performed with D-[3-^{3}H]glucose using a continuous insulin infusion of 3.5 mU/kg/min as previously described (54). HGP was assessed by subtraction of the glucose infusion rate from whole-body glucose turnover measured with D-[3-^{3}H]glucose.

In vivo insulin signaling. Following an overnight fast, mice were anesthetized with 2,2,2-tribromoethanol in PBS (Avertin) and injected with 5 U of regular human insulin (Novolin, Novo Nordisk) via the inferior vena cava. Five minutes after the insulin bolus, tissues were removed and frozen in liquid nitrogen. Immunoprecipitation and immunoblot analysis of insulin signaling molecules were performed using tissue homogenates prepared in a tissue homogenization buffer that contained 25 mM Tris-HCl (pH 7.4), 10 mM Na_3VO_4, 100 mM NaF, 50 mM $Na_4P_2O_7$, 10 mM EGTA, 10 mM EDTA, 2 mM phenylmethylsulfonyl fluoride, and 1% Nonidet-P40 supplemented with protease inhibitor cocktail (Sigma-Aldrich). All protein expression data were quantified by densitometry using NIH Image. Rabbit polyclonal anti-Akt, anti–phospho-Akt (Ser473), anti–phospho-SK3β (Ser9), anti-Foxo1, anti-GSK3, anti–phospho-p70S6K (Thr389), anti–phospho-p70S6K (Thr421/Ser424), anti-p70S6K, anti–lamin A/C, and anti-tubulin were purchased from Cell Signaling Technology. Anti-PKCδ, anti-SREBP1c, and anti–IRS-1 were purchased from Santa Cruz Biotechnology Inc. Anti-SOD4 was purchased from Abcam. Anti–phospho–IRS-1 (Ser307) was purchased from Upstate.

qPCR analysis. Total RNA was isolated from mouse tissues using an RNeasy kit (QIAGEN). cDNA was prepared from 1 μg of RNA using the Advantage RT-PCR kit (BD) with random hexamer primers, according to manufacturer's instructions. The resulting cDNA was diluted 10-fold, and a 5-μl aliquot was used in a 20-μl PCR reaction (SYBR Green, PE Biosystems) containing primers at a concentration of 300 nM each. PCR reactions were run in triplicate and quantitated in the ABI Prism 7700 Sequence Detection System. Ct values were normalized to level of ribosomal 18S RNA.

Leptin treatment. Male *ob/ob* mice (aged 6 weeks) and their lean *ob* control littermates were purchased from The Jackson Laboratory and acclimated to our animal facility for 2 weeks before study. Mice were implanted with osmotic pumps (1007D; Alzet) containing either PBS or recombinant mouse leptin (24 μg/d; National Hormone and Peptide Program, Harbor-UCLA Medical Center) for 4 days. Insulin-treated mice also received 4 subcutaneous bovine insulin pellets (LinBit, LinShin), a dose found to raise insulin levels in leptin-treated *ob/ob* mice to those found in untreated

ob/ob mice. Fasting insulin and glucose levels were obtained in a cohort of *ob/ob* mice by subjecting them to a 6-hour fast 2 days after initiation of treatment with leptin or insulin.

STZ diabetic mice. B6 mice at 6 weeks of age received either daily intraperitoneal injections of sodium citrate (pH 4.3) for controls or STZ (Sigma-Aldrich) resuspended in sodium citrate, 100 μg/g body weight for 3 consecutive days. When these mice achieved fed glucose levels of greater than 400 mg/dl for 3 consecutive days, they were separated into two equal groups. One group was not treated, while the other was treated with subcutaneous insulin pellets (LinShin), to obtain fed glucose levels of less than 200 mg/dl for at least 3 consecutive days. For PHZ treatment of diabetic mice, 8-week-old male B6 mice were treated with a single intraperitoneal injection (200 μg/g body weight) of STZ (Sigma-Aldrich). PHZ (Sigma-Aldrich) was dissolved in a solution containing 10% ethanol, 15% DMSO, and 75% saline and was injected subcutaneously at a dose of 0.4 g/kg twice daily for 10 days from 8 days after the STZ injection. Control mice were injected with the same volume of vehicle.

Inflammation and ER stress induction. To induce inflammation in vivo, we injected mice intraperitoneally with 100 μg LPS (*Escherichia coli* 55:B5; Sigma-Aldrich) or sterile saline as control. Mice were sacrificed 18 hours after injection. For ER stress studies, sibling mice (6–10 weeks old) were given a single 1-μg/g body weight intraperitoneal injection of a 0.05-mg/ml suspension of tunicamycin and sacrificed 2, 4, 6, and 8 hours after injection.

Genomic DNA extractions. Tail DNA was extracted with DNeasy Blood & Tissue Kit from QIAGEN. PKCδKO mice were genotyped with the following primers: PKCD-Fwd, 5′-gCTCTATTgCCTCggCTTCAT-3′; PKCD-R, 5′-AggTgAgAAgACAgCAAAggg-3′; LacZ-F, 5′-TgATgCggTgCTgATTACgAC-3′; LacZ-R, 5′-gTCAAAACAggCggCAgTAAg-3′. PKCδ floxed animals were genotyped with the following primers: primer F (Lox F3), 5′-CTgCTgggTAACTTAACAACAAgACC-3′; primer R (Lox R-101), 5′-CTgCTAAATAACATgATgTTCggTCC-3′; Prkcd flox recombination 1744, 5′-gTAgggTTggAAgggTCCCTAgA-3′.

Statistics. All results are expressed as mean ± SEM. Significance was established using the 2-tailed Student's *t* test and ANOVA when appropriate. Differences were considered significant at $P < 0.05$. Correlation studies were performed with Statview software (SAS Institute Inc.). For analysis of correlations between PKC expression and metabolic parameters in the human studies, Spearman rank correlations were performed.

Acknowledgments

The authors thank Michael Rourk and Graham Smith for animal technical assistance. This work was supported by the NIH grants DK31036 and DK33201, an American Diabetes Association mentor-based award, and the Mary K. Iacocca Professorship to C.R. Kahn.

Received for publication December 8, 2010, and accepted in revised form March 30, 2011.

Address correspondence to: C. Ronald Kahn, Joslin Diabetes Center and Harvard Medical School, One Joslin Place, Boston, Massachusetts 02215, USA. Phone: 617.732.2635; Fax: 617.732.2487; E-mail: c.ronald.kahn@joslin.harvard.edu.

1. Yu AS, Keeffe EB. Nonalcoholic fatty liver disease. *Rev Gastroenterol Disord*. 2002;2(1):11–19.
2. Singer JB, et al. Genetic dissection of complex traits with chromosome substitution strains of mice. *Science*. 2004;304(5669):445–448.
3. Colombo C, et al. Opposite effects of background genotype on muscle and liver insulin sensitivity of lipoatrophic mice. Role of triglyceride clearance. *J Biol Chem*. 2003;278(6):3992–3999.
4. Haluzik M, et al. Genetic background (C57BL/6J versus FVB/N) strongly influences the severity of diabetes and insulin resistance in ob/ob mice. *Endocrinology*. 2004;145(7):3258–3264.
5. Kulkarni RN, et al. Impact of genetic background on development of hyperinsulinemia and diabetes in insulin receptor/insulin receptor substrate-1 double heterozygous mice. *Diabetes*. 2003;52(6):1528–1534.
6. Almind K, Kahn CR. Genetic determinants of energy expenditure and insulin resistance in diet-induced obesity in mice. *Diabetes*. 2004;53(12):3274–3285.
7. Almind K, Kulkarni RN, Lannon SM, Kahn CR. Identification of interactive loci linked to insulin and leptin in mice with genetic insulin resistance. *Diabetes*. 2003;52(6):1535–1543.
8. Ravichandran LV, Esposito DL, Chen J, Quon MJ. Protein kinase C-zeta phosphorylates insulin receptor substrate-1 and impairs its ability to activate phosphatidylinositol 3-kinase in response to insulin. *J Biol Chem*. 2001;276(5):3543–3549.
9. Greene MW, Ruhoff MS, Roth RA, Kim JA, Quon MJ, Krause JA. PKCdelta-mediated IRS-1 Ser24 phosphorylation negatively regulates IRS-1 function. *Biochem Biophys Res Commun*. 2006;349(3):976–986.
10. Ishizuka T, et al. Protein kinase C (PKC) beta modulates serine phosphorylation of insulin receptor substrate-1 (IRS-1) — effect of overexpression of PKCbeta on insulin signal transduction. *Endocr Res*. 2004;30(2):287–299.
11. Lam TK, et al. Free fatty acid-induced hepatic insulin resistance: a potential role for protein kinase C-delta. *Am J PhysiolEndocrinol Metab*. 2002; 283(4):E682–E691.
12. Frangioudakis G, et al. Diverse roles for protein kinase C delta and protein kinase C epsilon in the generation of high-fat-diet-induced glucose intolerance in mice: regulation of lipogenesis by protein kinase C delta. *Diabetologia*. 2009;52(12):2616–2620.
13. She X, Cheng Z, Zollner S, Church DM, Eichler EE. Mouse segmental duplication and copy number variation. *Nat Genet*. 2008;40(7):909–914.
14. Formisano P, Beguinot F. The role of protein kinase C isoforms in insulin action. *J Endocrinol Invest*. 2001; 24(6):460–467.
15. Pihlajamaki J, et al. Thyroid hormone-related regulation of gene expression in human fatty liver. *J Clin Endocrinol Metab*. 2009;94(9):3521–3529.
16. Pihlajamaki J, et al. Cholesterol absorption decreases after Roux-en-Y gastric bypass but not after gastric banding. *Metabolism*. 2010;59(6):866–872.
17. Mori MA, et al. A systems biology approach identifies inflammatory abnormalities between mouse strains prior to development of metabolic disease. *Diabetes*. 2010;59(11):2960–2971.
18. Ozcan U, et al. Endoplasmic reticulum stress links obesity, insulin action, and type 2 diabetes. *Science*. 2004;306(5695):457–461.
19. Greene MW, Ruhoff MS, Burrington CM, Garofalo RS, Orena SJ. TNFalpha activation of PKCdelta, mediated by NFkappaB and ER stress, cross-talks with the insulin signaling cascade. *Cell Signal*. 2010;22(2):274–284.
20. Qi X, Mochly-Rosen D. The PKCdelta-Abl complex communicates ER stress to the mitochondria — an essential step in subsequent apoptosis. *J Cell Sci*. 2008;121(pt 6):804–813.
21. Leitges M, et al. Exacerbated vein graft arteriosclerosis in protein kinase Cdelta-null mice. *J Clin Invest*. 2001;108(10):1505–1512.
22. Dennis PB, Pullen N, Pearson RB, Kozma SC, Thomas G. Phosphorylation sites in the autoinhibitory domain participate in p70(s6k) activation loop phosphorylation. *J Biol Chem*. 1998;273(24):14845–14852.
23. Um SH, et al. Absence of S6K1 protects against age- and diet-induced obesity while enhancing insulin sensitivity. *Nature*. 2004;431(7005):200–205.
24. Puigserver P, et al. Insulin-regulated hepatic gluconeogenesis through FOXO1-PGC-1alpha interaction. *Nature*. 2003;423(6939):550–555.
25. Sampson SR, Cooper DR. Specific protein kinase C isoforms as transducers and modulators of insulin signaling. *Mol GenetMetab*. 2006;89(1–2):32–47.
26. Letiges M, et al. Knockout of PKCalpha enhances insulin signaling through PI3K. *Mol Endocrinol*. 2002;16(4):847–858.
27. Standaert ML, et al. Effects of knockout of the protein kinase C beta gene on glucose transport and glucose homeostasis. *Endocrinology*. 1999;140(10):4470–4477.
28. Farese RV, et al. Muscle-specific knockout of PKC-lambda impairs glucose transport and induces metabolic and diabetic syndromes. *J Clin Invest*. 2007; 117(8):2289–2301.
29. Sajan MP, et al. Role of atypical protein kinase C in activation of sterol regulatory element binding protein-1c and nuclear factor kappa B (NFkappaB) in liver of rodents used as a model of diabetes, and relationships to hyperlipidaemia and insulin resistance. *Diabetologia*. 2009;52(6):1197–1207.
30. Taniguchi CM, et al. Divergent regulation of hepatic glucose and lipid metabolism by phosphoinositide 3-kinase via Akt and PKClambda/zeta. *Cell Metab*. 2006;3(5):343–353.
31. Kim JK, et al. PKC-theta knockout mice are protected from fat-induced insulin resistance. *J Clin Invest*. 2004;114(6):823–827.
32. Gao Z, et al. Inactivation of PKCtheta leads to increased susceptibility to obesity and dietary insulin resistance in mice. *Am J Physiol Endocrinol Metab*. 2007;292(1):E84–E91.
33. Bowden DW, et al. Coincident linkage of type 2 diabetes, metabolic syndrome, and measures of cardiovascular disease in a genome scan of the diabetes heart study. *Diabetes*. 2006;55(7):1985–1994.
34. Jacob A, et al. The regulatory domain of protein kinase C delta positively regulates insulin receptor

signaling. *J Mol Endocrinol*. 2010;44(3):155–169.
35. Geraldes P, et al. Activation of PKC-delta and SHP-1 by hyperglycemia causes vascular cell apoptosis and diabetic retinopathy. *Nat Med*. 2009; 15(11):1298–1306.
36. Hennige AM, et al. Overexpression of kinase-negative protein kinase Cdelta in pancreatic beta-cells protects mice from diet-induced glucose intolerance and beta-cell dysfunction. *Diabetes*. 2010; 59(1):119–127.
37. Uchida T, et al. Protein kinase Cdelta plays a nonredundant role in insulin secretion in pancreatic beta cells. *J Biol Chem*. 2007;282(4):2707–2716.
38. Haas JT, Biddinger SB. Dissecting the role of insulin resistance in the metabolic syndrome. *Curr Opin Lipidol*. 2009;20(3):206–210.
39. Shimomura I, Matsuda M, Hammer RE, Bashmakov Y, Brown MS, Goldstein JL. Decreased IRS-2 and increased SREBP-1c lead to mixed insulin resistance and sensitivity in livers of lipodystrophic and ob/ob mice. *Mol Cell*. 2000;6(1):77–86.
40. Brown MS, Goldstein JL. Selective versus total insulin resistance: a pathogenic paradox. *Cell Metab*. 2008;7(2):95–96.
41. Li S, Brown MS, Goldstein JL. Bifurcation of insulin signaling pathway in rat liver: mTORC1 required for stimulation of lipogenesis, but not inhibition of gluconeogenesis. *Proc Natl Acad Sci U S A*. 2010;107(8):3441–3446.
42. Copps KD, Hancer NJ, Opare-Ado L, Qiu W, Walsh C, White MF. Irs1 serine 307 promotes insulin sensitivity in mice. *Cell Metab*. 2010;11(1):84–92.
43. Talior I, Yarkoni M, Bashan N, Eldar-Finkelman H. Increased glucose uptake promotes oxidative stress and PKC-delta activation in adipocytes of obese, insulin-resistant mice. *Am J Physiol Endocrinol Metab*. 2003;285(2):E295–E302.
44. Talior I, Tennenbaum T, Kuroki T, Eldar-Finkelman H. PKC-delta-dependent activation of oxidative stress in adipocytes of obese and insulin-resistant mice: role for NADPH oxidase. *Am J Physiol Endocrinol Metab*. 2005;288(2):E405–E411.
45. Wallerstedt E, Smith U, Andersson CX. Protein kinase C-delta is involved in the inflammatory effect of IL-6 in mouse adipose cells. *Diabetologia*. 2010;53(5):946–954.
46. Horovitz-Fried M, Jacob AI, Cooper DR, Sampson SR. Activation of the nuclear transcription factor SP-1 by insulin rapidly increases the expression of protein kinase C delta in skeletal muscle. *Cell Signal*. 2007;19(3):556–562.
47. Brand C, Horovitz-Fried M, Inbar A, Tamar-Brutman-Barazani, Brodie C, Sampson SR. Insulin stimulation of PKCdelta triggers its rapid degradation via the ubiquitin-proteasome pathway. *Biochim Biophys Acta*. 2010;1803(11):1265–1275.
48. Braiman L, et al. Insulin induces specific interaction between insulin receptor and protein kinase C delta in primary cultured skeletal muscle. *Mol Endocrinol*. 2001;15(4):565–574.
49. Braiman L, et al. Protein kinase Cdelta mediates insulin-induced glucose transport in primary cultures of rat skeletal muscle. *Mol Endocrinol*. 1999; 13(12):2002–2012.
50. Brand C, Cipok M, Attali V, Bak A, Sampson SR. Protein kinase Cdelta participates in insulin-induced activation of PKB via PDK1. *Biochem Biophys Res Commun*. 2006;349(3):954–962.
51. Oriente F, et al. Protein kinase C-alpha regulates insulin action and degradation by interacting with insulin receptor substrate-1 and 14-3-3 epsilon. *J Biol Chem*. 2005;280(49):40642–40649.
52. Samuel VT, et al. Inhibition of protein kinase Cepsilon prevents hepatic insulin resistance in nonalcoholic fatty liver disease. *J Clin Invest*. 2007; 117(3):739–745.
53. Taniguchi CM, et al. The p85alpha regulatory subunit of phosphoinositide 3-kinase potentiates c-Jun N-terminal kinase-mediated insulin resistance. *Mol Cell Biol*. 2007;27(8):2830–2840.
54. Norris AW, et al. Muscle-specific PPARgamma-deficient mice develop increased adiposity and insulin resistance but respond to thiazolidinediones. *J Clin Invest*. 2003;112(4):608–618.